Oblique shock wave effects on biological membranes

Damiani SOURMAIDOU[1], Stephanie DUFOURMANTELLE[1], Nikolaos ASPROULIS[1,*], Dimitris DRIKAKIS[1,2], Sandip PAL[3]

* Corresponding author: Tel.: ++44 (0)1234 758207; Fax: ++44 (0)1234 754635; Email: n.asproulis@cranfield.ac.uk

1 Fluid Mechanics and Computational Science Department, Cranfield University, UK
2 The Cyprus Institute, Computation-based Science and Technology Research Center, Cyprus
3 Broomfield Hospital, Chelmsford, United Kingdom

Abstract In the present study the effects of oblique shock waves on the lateral diffusion coefficients of a 1-palmitoyl-2-oleoyl-*sn*-glycero-3-phosphocholine (POPC) biological membranes through molecular dynamics simulations are being under examination. Computational simulations have been carried out by utilising the NPT ensemble with shock impulses varying from 0.33mPa s to 100mPa s. The applied incident angles vary between 0° and 80° corresponding to the perpendicular and almost tangential case respectively. It is shown that the membrane thickness gets thinner under the application of a shock. The area per lipid is also reduced, while the volume increases in the beginning of the application of the shock and afterwards it reduces until it gets to the same values that correspond to the equilibrium state.

Keywords: Shock wave, biological membrane, molecular dynamics, diffusion coefficient, incident angle, mass transport

1. Introduction

Every year more than 8 million people die due to cancer, making it a leading cause of death in the Western World (Ruddon, 2007). Thus, efforts to establish new methods that improve drug delivery and efficiency have been increased. Cancer treatment research involves various methods, from the development of vaccines to the use of advanced surgical procedures. The effectiveness of the treatment lies on the suitability of the pharmacological compound and its delivery to the desired pathological area. Therefore, scientists have been researching techniques to increase drug absorption into the cell cytoplasm, via generating transient permeabilisation of the cell membrane (Kodama *et al*., 2000). This transfusion can be induced using two different methods. The first one alters the composition of lipids in the lipid bilayer with the introduction of detergents (Schafer *et al*., 1987), bacterial toxins (Spiller *et al*., 1998), or virus-mediated fusogenic lyposomes (Kaneda,

1999). A second method applies electric fields (Ho *et al*., 1996), ultrasounds (Liu *et al*., 1998; Miller *et al*., 1999), or shock waves (Gambihler *et al*., 1994; Delius and Adams, (1999); Lee and Doukas (1999); Zhu *et al*., 2004).

Experimental procedures when applied to micro and nano scales are usually associated with financial burden and technical difficulties in obtaining accurate measurements. Therefore, the scientific community has embraced computational tool as a viable approach for performing complementary studies on biological systems aiming at establishing ways to enhance drug diffusion through the cell membrane. A computational approach that has been applied towards that direction is Molecular Dynamics (MD).

In the current study, MD is employed to investigate the effects of shock impulses on bio-membranes and study the membranes' responses. A number of properties related to the membrane are monitored such as membrane's thickness, area per lipid, and lateral diffusion.

2. Simulation Method

MD solves the Newtonian equation of motion for each atom of the system (Phillips *et al*., 2005):

$$m_\alpha \ddot{\vec{r}}_\alpha = -\frac{\partial}{\partial \vec{r}_\alpha} U_{total}(\vec{r}_1,..,\vec{r}_N), \quad \alpha = 1, 2 \dots N \quad (1)$$

where m, is the mass of an atom α, $\vec{r}$, denotes the position of atom α, and ,U$_{total}$, stands for the total potential energy which depends on the positions of all atoms thus couples their motion. The dynamics of all particles is known for every time step and the potential energy function is given as part of the force field functions:

$$U_{total} = U_{bond} + U_{angle} + U_{dihedral} + U_{vdW} + U_{Coulomb} \quad (2)$$

The first three terms express the stretching, bending, and torsional bonded interactions and the last two, the non-bonded interactions between pairs of atoms in the system; the van der Waal's forces and the electrostatic interactions.

2.1 Shock wave implementation

For the current study the shock wave's strength is provided through its impulse which is defined as follows (Kodama *et al*., 2000):

$$I = \int_0^{T_{I_p}} P \, dt \quad (3)$$

where P is the instant pressure while the impulse is being applied and T_{I_p}, the duration.

The shock waves applied on the POPC membrane have been modelled as a rise in the momentum of the upper water layer that was under the effect of the shocks. The new velocities that the water molecules of the upper layer will have are determined by the incident angle *θ*, the impulse, and the thickness of the shock. The velocities of the molecules are calculated as:

$$v = \frac{I_p * A}{m * N_w} \quad (4)$$

where A is the area in the XY plane of the membrane, $m = 2.99146 * 10^{-26} kg$ is the

mass of a water molecule, and N_w is the number of water molecules in the water slab dictated by the thickness of the shock wave impact, T_{sw}. Accordingly, the volume of the water slab will be:

$$V_{water\ slab} = T_{sw} * A \quad (5)$$

The incident angle θ determines the impulse value which is decomposed into perpendicular components as shown below:

$$I_p = \begin{cases} I_{p,y} = I_p \sin\theta \\ I_{p,z} = I_p \cos\theta \end{cases}$$

In the current study the incident angle was implemented in directions z and y. Alternatively, the impulse could have been projected onto axis z and x.
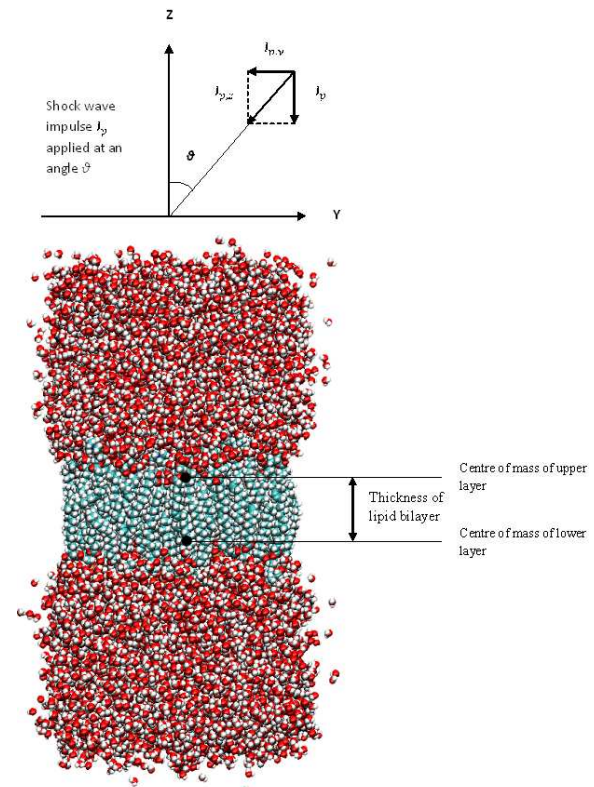

Figure 1. Schematic of biological membrane along with the applied oblique shock wave

2.2 Calculation of lateral diffusion

The diffusion coefficient has been calculated by first utilising the formula of Einstein about the mean square displacement (MSD) of the lipids (Karniadakis, 2004):

$$MSD = \langle \frac{1}{N_L} \sum_{i=1}^{N_L} [r_i(t) - r_i(0)]^2 \rangle \quad (6)$$

where N_L is the number of lipids, $r_i(t)$ the position of the lipid i at time t, with the symbol $\langle \ \rangle$ denoting an average of the timesteps and/or particles.

The diffusion coefficient D is expressed as the slope of the mean square displacement, which in three dimensions is:

$$D = \frac{1}{6}\lim_{t \to \infty} \frac{d}{dt}(MSD) \quad (7)$$

As the current study measures the lateral diffusion of the lipids in the XY plane, the formula has been modified for the case of two dimensions:

$$D = \frac{1}{4}\lim_{t \to \infty} \frac{d}{dt}(MSD) \quad (8)$$

2.3 Computational Setup

The biological membrane employed consists of 104 1-palmitoyl-2-oleoyl-*sn*-glycero-3-phosphocholine (POPC) phospholipids with 52 lipids on the upper layer and 52 lipids on the lower one. It is in the *cis* unsaturated form and has been hydrated with water molecules on top of the hydrophilic heads of both monolayers. This results to a total number of 15134 water molecules and 59338 atoms being employed for the modeling of the complete system.

The computational box spans for 66.2Å, 65.0Å, and 155.9Å across the x, y and z direction with periodic boundary conditions to have been applied in each direction respectively. The system is initially minimized to the minimum energetic stage and integrated for 45ps through the NPT ensemble until equilibration is achieved. The pressure and temperature remain constant through the simulation equal to 1atm and 310K. The time-step used is 1fs with non-bonded interactions have been calculated every 2fs and full electrostatics every 4fs. The total simulation time is 200ps.

The shock impulse applied varied between 0.33mPa s and 100mPa s, while the thicknesses of the impulses were 5Å, 7Å, 10Å, and 12Å. The incident angle varied between 0° and 80°. The simulations have been performed through the NPT ensemble in order to examine the different response of the membrane to the different ensembles.

3. Results and Discussion

The membrane-water system is initially minimized and equilibrated for a total time equal to 50ps. During the first 1ps for the minimization procedure takes place followed by 1ps where the values of temperature increase up to 310K, 3ps where values of pressure increase up to 1atm and 45ps until the volume is equilibrated. Figure 2 shows a snapshot of the entire system after minimization and equilibration.
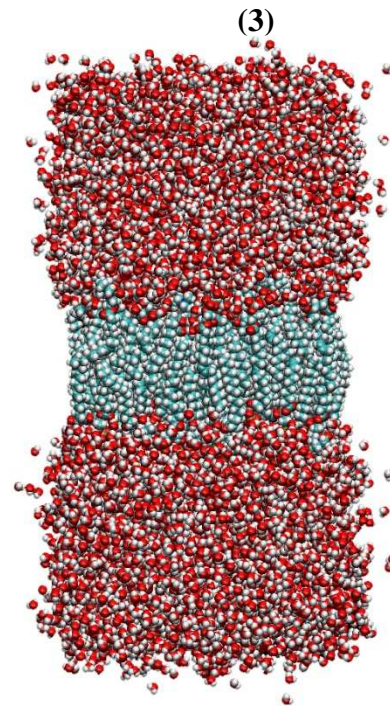

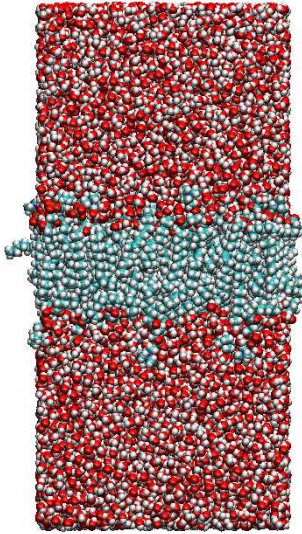**Figure 2.** Snapshot of POPC bilayer after minimization and equilibration

.

Figure 3. POPC bilayer after the application of a shock wave impulse of 0.99mPa s and thickness 7Å from an incident angle of 50°

3.1 Shock wave thickness effect

Aiming to study the effect of shock wave thickness a number of simulations with various thicknesses and impulses initially for the 0 incidence angle are examined. More specifically, shock wave thicknesses used span from 5Å to 12 Å.
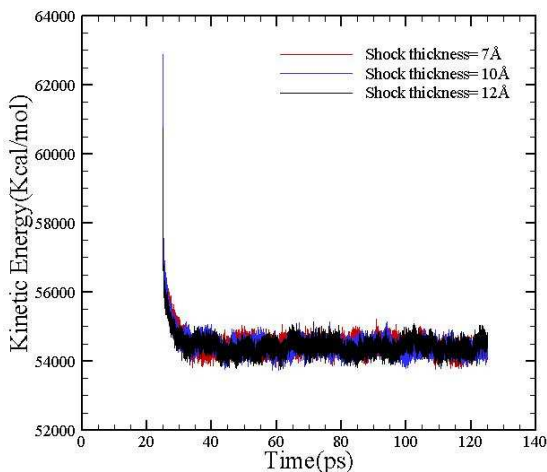

Figure 4. Kinetic energy of the system for impulse 4mPa s and at various shock wave thicknesses

Figure 4 shows the time variation of the system's kinetic energy for various values of shock's thickness and impulse 4mPa s. A common element observed is a rapid increase in the kinetic energy the time that the shock is introduced to the system (t=25ps). As the simulation evolves the kinetic energy for all

values of shock's thickness decreases through the NPT integrator's temperature controller and relaxes almost to the same mean value for the various thicknesses. The rapid increase to the system's energy was expected since through the application of the shock wave essentially additional momentum and consequently kinetic energy is introduced to the system. As the shock's thickness increases a small decrease to the maximum kinetic energy can be identified. The thickness of the shock does not alter the total momentum transferred to the system, which is determined by the impulse, but it mainly affects the velocity distribution across the water molecules. To further elaborate, larger thickness implies that the shock will be applied to larger number of water molecules increasing therefore the total mass and as a consequence a reduced velocity is applied (see Equation 4).
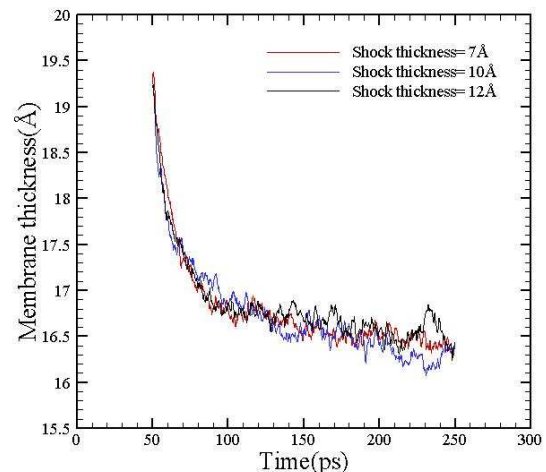

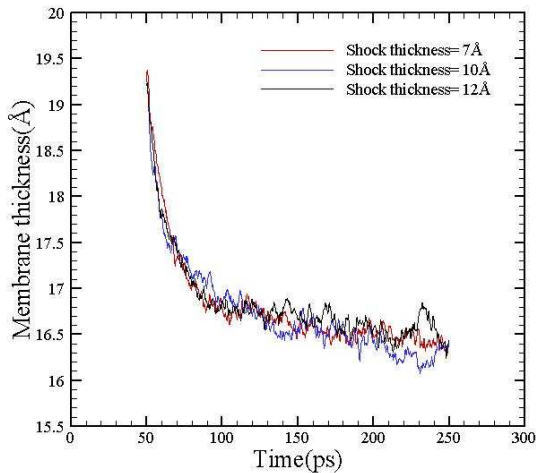**Figure 5.** Thickness of the membrane for impulse 4mPa s and shock wave thickness 10Å

In

Figure 5 the time variation of membrane's thickness for impulse 4mPa s and for three values of shock's thicknesses is presented. At the beginning of the simulation after minimization and equilibration the thickness of the membrane is the same for the examined cases and a common trend is noticed with the membrane's thickness to decrease until a local equilibrium is reached. Although, small differences between the different shocks exist, it can be observed that towards the end of the simulation the minimum membrane thickness is obtained for shock length equal to 10 Å. This is mainly linked to the efficiency of the momentum transfer across the water membrane interface. Smaller values of shock's length imply that the mechanism for momentum exchange is based on larger water velocities and small application time whereas larger values of shock's length mean that a shock with smaller velocity will hit the membrane for a longer period of time.

In Figure 6 the corresponding movement of membrane's center of mass for impulse 4mPa s and for various values of shock's thickness is presented. As expected for smaller values of thickness the center of mass (COM) remains closer to its original position whereas for higher values a larger disparity is noticed. Smaller thickness implies a smaller application time for the shock and therefore the COM remains in the vicinity of its original place.
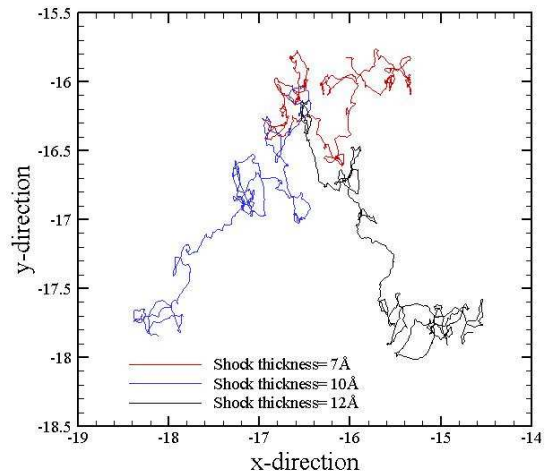

Figure 6. Centre of mass of the membrane for impulse 4mPa s and at various shock wave thicknesses
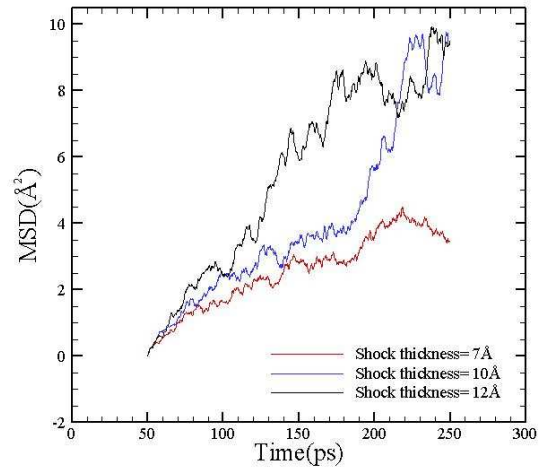

Figure 7 shows the mean square displacement of the lipids in the membrane as function of time for different shock's thicknesses. The slope of the MSD is linked with the diffusion of the lipids and larger slopes imply higher lipid mobility within the membrane. For the specific case larger slope in total is noticed for thickness 10 Å and smaller for 7 Å. The MSD slopes and therefore the lipid's diffusivity are dependent on the efficiency of the momentum transferred from the water molecules to the upper layer of the membrane. More efficient momentum transfer implies higher slopes and consequently larger diffusion coefficients.
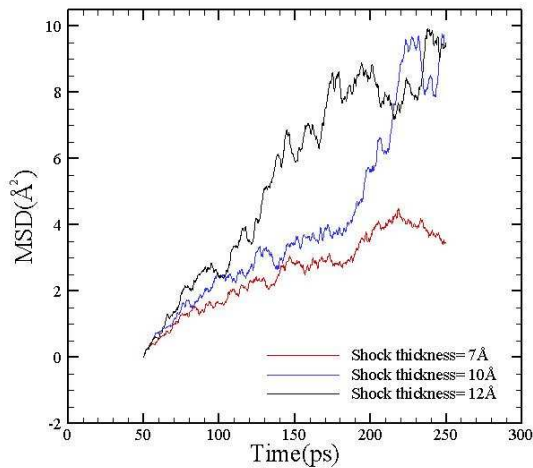
Figure 7. MSD of the membrane for impulse 4mPa s and at various shock wave thicknesses
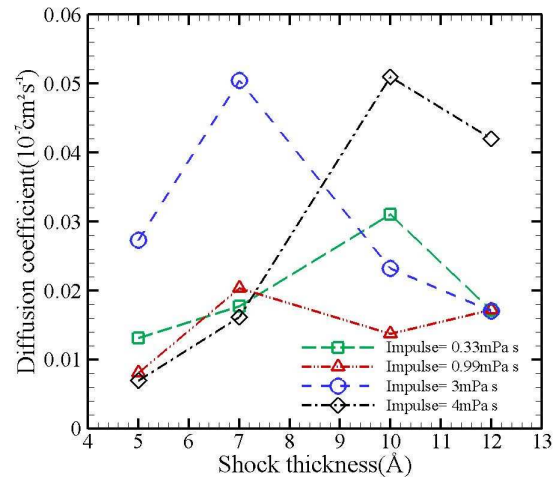

Figure 8. Diffusion coefficient as function of thickness at various impulses for 0° angle

3.2 Incidence angle effect

Additional computations have been carried out to study the effects of the incidence angle of the shock to the membrane system. As the oblique shock wave is applied momentum components are introduced to the system not only perpendicular to the membrane but also parallel to its surface. Although in absolute terms the perpendicular component of the impulse is reduced leading in principle to small diffusion coefficient values (Drikakis *et al.*, 2009), the parallel component is anticipated to increase the lateral mobility of the lipids enhancing therefore the lateral diffusion.

Figure 9 shows the kinetic energy of the water-membrane system as function of time for different incidence angles and shock's impulse and thickness 0.99mPa s and 5Å respectively. Similar to Figure 4, the kinetic energy is increased at the time the shock is introduced and as the simulation evolves any excessive heat generated from the additional kinetic energy is dissipated through the applied Nose-Hoover thermostats. The variations of the incidence angle do not alter the total kinetic energy introduced but mainly affect the distribution of the energy along the perpendicular and longitudinal direction. As a consequence, smaller values of the incidence angle result in larger parallel to the membrane velocity components. Due to the presence of periodic boundary conditions additional time
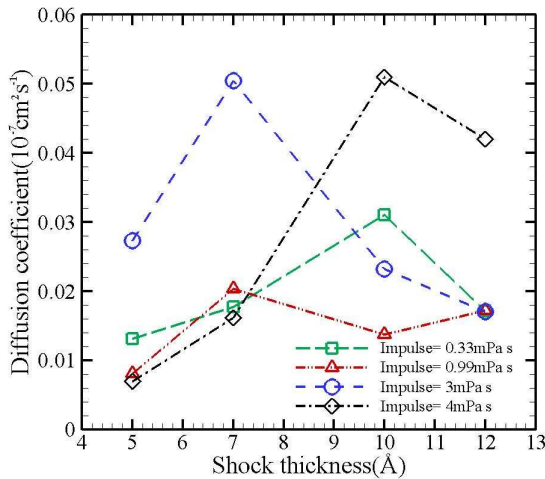

Figure 8 summarises the diffusion coefficient values as function of shock's thickness for different impulse values. It can be seen that for all different values of impulse, that corresponds to different values of momentum, the lateral diffusion coefficient initially increases as the shock's thickness is increased until a maximum is achieved. The maximum corresponds to the optimum scenario for the momentum to be transported in the membrane. Following the maximum and as the shock's thickness continuous to increase the efficiency of momentum transfer drops and the values of the diffusion coefficient drop accordingly.

is required for the energy to be dissipated resulting in slightly larger oscillations, around the mean kinetic energy, for the smaller angle (see Figure 9).

Figure 10 shows the membrane's thickness as function of time for incidence angle 20°, 30° and 40°. The same behavior is noticed for all three incidence angles examined, with the membrane to shrink after the application of the oblique shock, with a reduced rate until relaxes to a local equilibrium state. The trend for the various angles is almost identical with minor differences being noticed in the initial decrease rate of the membrane's thickness. More specifically, larger decrease rate is noticed for the smaller incidence angle due to the presence of larger perpendicular to the membrane velocity components.
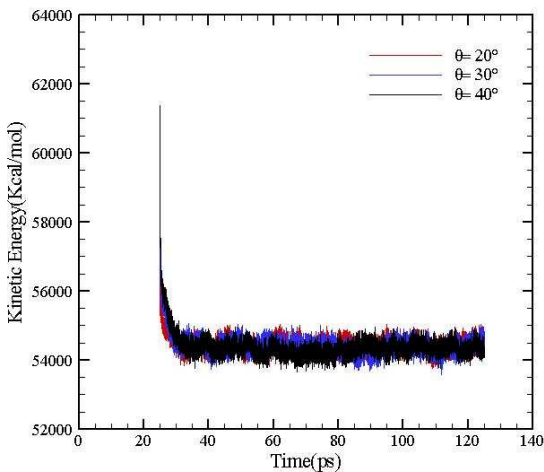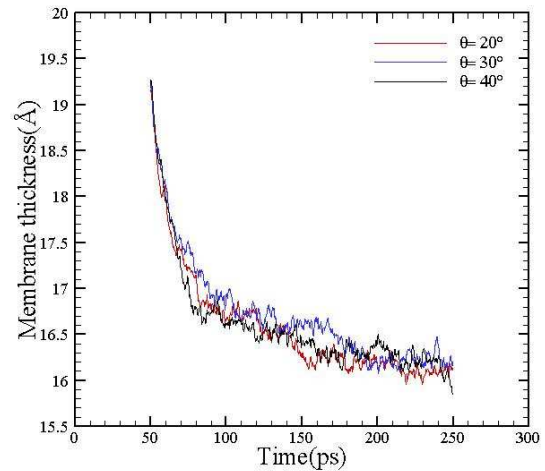

Figure 10. Thickness of the membrane for shock wave thickness 5Å and impulse 0.99mPa s for various incidence angles

Figure 11 shows the positions of the center of membrane's mass during the simulating time. It can be seen that as the incidence angle increases, the longitudinal to the membrane momentum component increases enhancing therefore the mobility of the COM. As seen in Figure 11 the spectrum of the COM's x and y coordinates is increasing in a non linear fashion as the incidence angle increases from 20° to 30° and from 30° to 40°. For the smaller angle 20° the longitudinal velocity components are smaller causing the membrane's COM to slightly oscillate along its original y position.

Figure 9. Kinetic energy of the membrane for shock wave thickness 5Å and impulse 0.99mPa s for various incidence angles
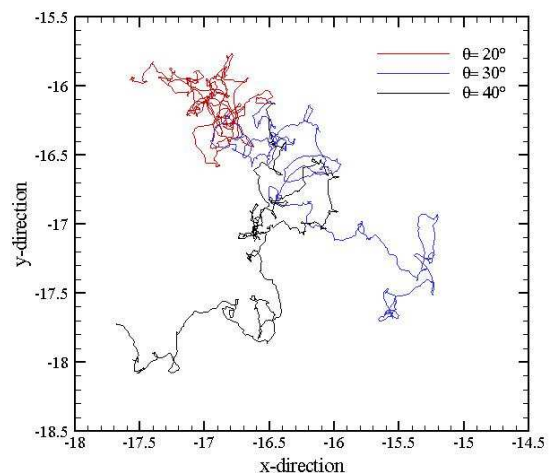

Figure 11. Centre of mass of the membrane for shock wave thickness 5Å and impulse 0.99mPa s for various incidence angles

Figure 12 shows the mean square displacement of the membrane's lipids as function of time for a shock with thickness 5 Å and three incidence angles 20°, 30° and 40°. There is a significant dependence of the MSD from the incidence angle with the MSD slope to continuously increasing in a non-linear manner as the angle increases from 20° to 40°. The aforementioned increase to the slope corresponds to higher lateral diffusion figures as shown in Figure 13.
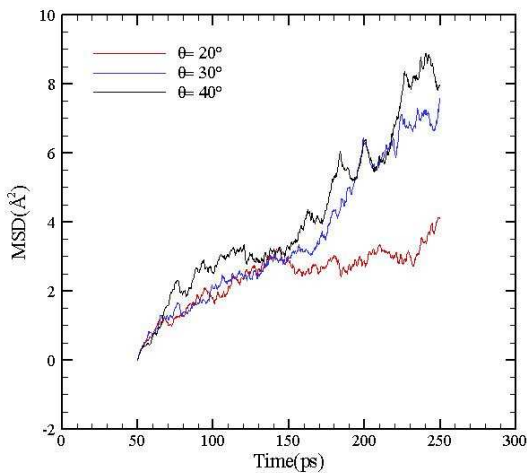

Figure 12. MSD of the membrane as function of time for shock wave thickness 5Å and impulse 0.99mPa s for various incidence angles

A similar trend is noticed for all three impulses with the diffusion coefficient initially being significantly increased as the incidence angle increases followed by a global maximum and then entering a decreasing phase with slight fluctuations around a certain value. As the oblique shock's angle initially increases the parallel to the membrane momentum components increase enhancing therefore the lateral mobility of the lipids belonging to the top layer of the membrane. The increased mobility of the lipids is reflected to corresponding increments of the diffusion coefficient values. However, if the angle of attack continues to increase the perpendicular to the membrane shock's velocity becomes weaker loosing increasing therefore the time needed for the wave to hit the membrane and reducing the amount of direct momentum transfer between the shock's water molecules

and the membrane's lipids. Furthermore, although the parallel velocity components are expected to continue to enhance the lateral particles' mobility, the increase rate is bounded by the effectiveness of the momentum transfer across the interface. As a consequence it just compensates any losses arising from perpendicular component leading therefore to almost constant values of diffusion.
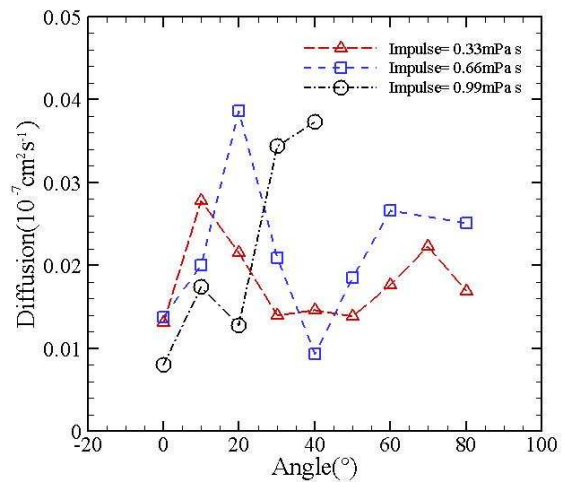

Figure 13. Diffusion coefficient as function of incidence angle at various impulses for shock wave thickness 5Å

4. Conclusions

In the present study attention has been drawn to the effects of oblique shock waves to the lateral diffusion coefficient of a POPC membrane. As the incidence angle is introduced an initial increase to the diffusion is observed due to the increase of the parallel to the wall shock's velocity components. Another characteristic of the shock wave that affects the amount of momentum propagated from the water molecules to the membrane is the shock thickness. As the thickness of the shock becomes larger the diffusion coefficient initially increases until a maximum value is obtained followed by a small decay.

In conclusion, additional studies have to be performed aiming to study the response of

more complicated membrane models where proteins are also considered. Defining the self diffusion coefficients of the surface proteins will have a great contribution towards a better understanding of mechanisms for optimising the drug delivery and drug adsorption.

References

Delius, M. and Adams, G. (1999), "Shock wave permeabilization with ribosome inactivating proteins: A new approach to tumor therapy", *Cancer Research,* vol. 59, no. 20, pp. 5227-5232.

Drikakis, D., Lechuga, J., and Pal, S. (2009). Effects of shock waves on biological membranes: A molecular dynamics study. *Journal of Computational and Theoretical Nanoscience, 6*(7), 1437-1442

Gambihler, S., Delius, M. and Ellwart, J. W. (1994), "Permeabilization of the plasma membrane of L1210 mouse leukemia cells using lithotripter shock waves", *Journal of Membrane Biology,* vol. 141, no. 3, pp. 267-275.

Ho, S. Y. and Mittal, G. S. (1996), "Electroporation of cell membranes: A review", *Critical Reviews in Biotechnology,* vol. 16, no. 4, pp. 349-362.

Kaneda, Y. (1999), "Development of a novel fusogenic viral liposome system (HVJ-liposomes) and its applications to the treatment of acquired diseases", *Molecular Membrane Biology,* vol. 16, no. 1, pp. 119-122.

Karniadakis, G. (2004), "10 Simple Fluids in Nanochannels 10.3 Diffusion Transport", in *Microflows and Nanoflows: Fundamentals and Simulation,* 2nd ed, Springer, New York, pp. 375.

Kodama, T., Hamblin, M. R. and Doukas, A. G. (2000), "Cytoplasmic molecular delivery with shock waves: Importance of impulse", *Biophysical journal,* vol. 79, no. 4, pp. 1821-1832.

Koshiyama, K., Kodama, T., Yano, T. and Fujikawa, S. (2008), "Molecular dynamics simulation of structural changes of lipid bilayers induced by shock waves: Effects of

incident angles", *Biochimica et Biophysica Acta - Biomembranes,* vol. 1778, no. 6, pp. 1423-1428.

Lee, S. and Doukas, A. G. (1999), "Laser-generated stress waves and their effects on the cell membrane", *IEEE Journal on Selected Topics in Quantum Electronics,* vol. 5, no. 4, pp. 997-1003.

Liu, J., Lewis, T. N. and Prausnitz, M. R. (1998), "Non-invasive assessment and control of ultrasound-mediated membrane permeabilization", *Pharmaceutical Research,* vol. 15, no. 6, pp. 918-924.

Miller, D. L., Bao, S. and Morris, J. E. (1999), "Sonoporation of cultured cells in the rotating tube exposure system", *Ultrasound in Medicine and Biology,* vol. 25, no. 1, pp. 143-149.

Phillips, J. C., Braun, R., Wang, W., Gumbart, J., Tajkhorshid, E., Villa, E., Chipot, C., Skeel, R. D., Kalé, L. and Schulten, K. (2005), "Scalable molecular dynamics with NAMD", *Journal of Computational Chemistry,* vol. 26, no. 16, pp. 1781-1802.

Ruddon, R. W. (2007), *Cancer Biology,* 4th ed, Oxford University Press, New York.

Schafer, T., Karli, U. O., Gratwohl, E. K. -., Schweizer, F. E. and Burger, M. M. (1987), "Digitonin-permeabilized cells are exocytosis competent", *Journal of Neurochemistry,* vol. 49, no. 6, pp. 1697-1707.

Spiller, D. G., Giles, R. V., Grzybowski, J., Tidd, D. M. and Clark, R. E. (1998), "Improving the intracellular delivery and molecular efficacy of antisense oligonucleotides in chronic myeloid leukemia cells: A comparison of Streptolysin-O permeabilization, electroporation, and lipophilic conjugation", *Blood,* vol. 91, no. 12, pp. 4738-4746.

Zhu, S., Dreyer, T., Liebler, M., Riedlinger, R., Preminger, G. M. and Zhong, P. (2004), "Reduction of tissue injury in shock-wave lithotripsy by using an acoustic diode", *Ultrasound in Medicine and Biology,* vol. 30, no. 5, pp. 675-682.